Available online at http://scik.org
Commun. Math. Biol. Neurosci. 2026, 2026:41
https://doi.org/10.28919/cmbn/9842
ISSN: 2052-2541

A DYNAMIC COMPARTMENTAL MODEL FOR OPTIMIZING LEAK DETECTION IN WATER DISTRIBUTION SYSTEMS

AICHA TAYABE*, IMANE ELBERRAI, KHALID ADNAOUI

Laboratory of Analysis Modeling and Simulation (LAMS), Faculty of Sciences Ben M'Sik, Hassan II University of Casablanca, Morocco

Abstract. Water distribution systems face significant challenges from leaks that lead to substantial water losses and increased maintenance costs. Traditional detection methods often fall short in addressing the dynamic nature of pipe degradation and leak propagation. This paper introduces a novel compartmental approach inspired by epidemiological models, categorizing pipes into three states: intact, leaking, and repaired. We analyze equilibrium points and stability to identify critical thresholds for leak control and propose optimal strategies for preventive and repair efforts. Numerical simulations validate the theoretical findings, demonstrating the model's effectiveness in guiding maintenance decisions. This innovative methodology offers a new framework for optimizing resource allocation and improving the resilience of water distribution systems.

Keywords: water distribution systems; compartmental model; leak detection; stability analysis; optimal control.

2020 AMS Subject Classification: 34D20, 49J15, 49N90, 92D30.

1. INTRODUCTION

Water distribution networks form the vital arteries of modern civilization, essential for public health, economic stability, and environmental sustainability. Yet beneath our cities, a silent

*Corresponding author
E-mail address: aicha01tayabe@gmail.com
Received February 24, 2026

crisis unfolds: the widespread and persistent problem of water leakage. While essential for planning, traditional leak detection methods—often relying on acoustic sensors, ground-penetrating radar, or passive supervisory control and data acquisition (SCADA) systems—struggle to capture the complex, dynamic nature of how leaks initiate, propagate, and interact across a network [20]. As noted in recent infrastructure resilience studies, conventional monitoring approaches typically provide localized snapshots rather than system-wide dynamic behavior [21]. These methods excel at locating individual failures but offer limited insight into emergent network vulnerability patterns or long-term deterioration dynamics, a limitation highlighted in urban infrastructure analytics literature [22].

The challenge is further compounded by what engineering systems researchers have termed the "cascade effect" in networked infrastructure, where localized failures can trigger disproportionate system-wide consequences [23]. As infrastructure ages and operational demands intensify, a paradigm shift is needed—from reactive detection to predictive, systemic management.

Unexpectedly, a powerful solution may lie in the field of epidemiology. For nearly a century, compartmental models like the seminal Susceptible-Infectious-Recovered (SIR) framework by Kermack and McKendrick [2] have enabled researchers to understand and forecast the spread of diseases within populations. The conceptual parallel is striking: just as pathogens spread through social networks, pipe failures can propagate through infrastructure networks, influenced by adjacency, pressure conditions, and material susceptibility. This analogy has begun to inspire cross-disciplinary applications, yet its potential remains largely untapped in water infrastructure management, where most models focus on hydraulic simulation rather than failure dynamics.

Prior research has laid crucial groundwork for understanding water loss management. Foundational principles for water loss assessment and control were established in early handbooks and standards [12, 16], while comprehensive reviews have systematically cataloged available leakage management technologies and highlighted the growing role of advanced simulation [3]. From a methodological perspective, mathematical frameworks for optimal control have been successfully applied to diverse fields ranging from disease management to resource allocation

[18], yet their application to leak propagation remains notably underexplored. Recent case studies from operational environments, such as the integrated monitoring system in Casablanca [11], demonstrate the value of data-driven approaches but also reveal a persistent gap: the absence of a unified mathematical framework capable of both explaining and controlling leak dynamics across entire networks.

This paper fills that gap by introducing a novel epidemiological framework adapted specifically for water distribution systems. We develop a dynamic compartmental model that not only categorizes pipes into states of integrity but also incorporates the core mechanisms of failure propagation and recovery. Our approach moves beyond descriptive modeling to offer actionable insights through three key contributions:

First, we establish a fundamental threshold parameter—the basic reproduction number for leaks, R_0—which serves as a powerful diagnostic tool, predicting whether a network will naturally recover from leaks or descend into a state of persistent failure.

Second, we formulate an optimal control strategy that determines the most cost-effective allocation of resources between preventive maintenance (reducing failure spread) and reactive repairs (accelerating recovery), providing utilities with a scientifically grounded approach to budget allocation and intervention planning.

Finally, we validate our framework through comprehensive numerical simulations that not only verify theoretical predictions but also demonstrate tangible improvements over conventional approaches, showing significant reductions in both leak duration and volume.

In the sections that follow, we present the model formulation and equilibrium analysis (Section 2), establish local and global stability criteria (Sections 4–5), develop the optimal control framework (Section 6), and present numerical validation (Section 7). By bridging epidemiology and infrastructure engineering, this research provides both a theoretical foundation and practical methodology for transforming leak management from reactive patchwork to predictive, systematic stewardship of our critical water resources.

2. Model Description

Water leaks in distribution systems are a constant concern for those in charge of managing them. These leaks raise operating costs, lead to unnecessary water losses, and gradually

weaken the infrastructure. Recent studies show that more than 30% of treated water is lost due to leaks [1], which threatens the reliability of water services and highlights the necessity of developing systematic approaches for leakage detection and long-term control [3].

This study introduces a dynamic model inspired by an unexpected source: epidemiology. Much like the SIR model tracks how diseases spread through populations [2], we've adapted this approach to water networks by categorizing pipes into three interconnected states. On one end, we have intact pipes (P_b)—still functional but gradually weakening under daily stress. At the other extreme are leaking pipes (P_f), where water escapes relentlessly, straining the entire system. Bridging these states are repaired pipes (P_r), temporarily fixed but never fully immune to future failures.

This approach is both practical and effective. Leaks, like pathogens, follow predictable patterns: they exploit weak points, spread under pressure, and recur if not fully resolved. By translating these dynamics into mathematical terms, we give utilities a powerful new lens to predict leaks before they erupt, transforming reactive maintenance into proactive prevention.

In this study, the evolution of the water distribution network is modeled by considering several key processes. First, new intact pipes are introduced into the system at a rate λ, reflecting network expansions or the replacement of segments that have been removed. This mechanism ensures the continuous renewal of the infrastructure and supports the system's capacity to meet growing demands.

Intact pipes deteriorate naturally over time at a rate α, due to the combined effects of material aging, internal pressure stresses, and corrosion. Additionally, a fraction of these pipes is removed preemptively at a rate γ, as part of preventive maintenance programs. These interventions are designed to eliminate pipes that, while still functional, exhibit hidden weaknesses, advanced aging, or are made of materials deemed obsolete or hazardous, such as lead. By removing these vulnerable pipes before any failure occurs, network reliability and water quality can be preserved.

Leak propagation is modeled through the nonlinear interaction term $\beta P_b P_f$, which represents how the presence of leaking pipes accelerates the degradation of adjacent intact ones. This

interaction can be attributed to localized pressure variations, the corrosive action of escaping water, or the destabilization of surrounding soils.

Once leaks are present, a fraction of the leaking pipes is detected and assessed. Among these, some are judged irreparable and removed from the network at a rate θ, ensuring that severely damaged components do not persist in service. The remainder of the leaking pipes is repaired at a rate δ, after which they are transferred to the compartment of recovered pipes. However, repaired pipes are not immune to future failures: they may deteriorate again and be permanently removed from the network at a rate μ, particularly if the repair did not fully address underlying structural weaknesses.

The dynamics of the system are described by the following set of equations:

$$\dot{P}_b = \lambda - (\gamma + \alpha)P_b - \beta P_b P_f \tag{1}$$

$$\dot{P}_f = \beta P_b P_f - (\delta + \theta)P_f \tag{2}$$

$$\dot{P}_r = \delta P_f - \mu P_r \tag{3}$$

These equations model the transitions between states according to the parameters listed below:

Parameter	**Interpretation**	**Description**
λ	Addition of new pipes	Introduces new intact segments into the network.
α	Natural degradation	Rate at which intact pipes deteriorate over time.
γ	Planned removal of intact pipes	Rate at which intact pipes are proactively removed from the network (due to aging, hidden defects, or preventive replacement).
β	Leak propagation	Influence of leaking pipes on the deterioration of neighboring pipes.
δ	Repair of leaks	Rate at which leaking pipes are repaired and transferred to the repaired compartment.
θ	Abandonment of detected leaks	Rate at which detected leaking pipes are deemed irreparable and permanently removed from the network.
μ	Relapse	Rate at which repaired pipes develop leaks again.

TABLE 1. Description of the model parameters

3. Model Validity and Equilibrium Analysis

3.1. Validity of the Model.

Theorem 3.1.1. *All solutions of the model with non-negative initial conditions remain non-negative and bounded for all $t > 0$.*

Proof. We show that the proposed compartmental system is physically meaningful, in the sense that all its solutions remain non-negative for all $t > 0$. This is essential for any model that describes the proportions of pipes in a water distribution network.

Let us consider the positively invariant set defined by:

$$\mathbb{R}^3_+ = \left\{ (P_b, P_f, P_r) \in \mathbb{R}^3 \,\middle|\, P_b \geq 0, P_f \geq 0, P_r \geq 0 \right\},$$

and demonstrate that any solution starting in this set remains within it for all $t > 0$. Indeed, for any solution $(P_b(t), P_f(t), P_r(t)) \in \mathbb{R}^3_+$, we have:

$$\dot{P}_b\big|_{P_b=0} = \lambda > 0 \quad \text{for all } \lambda > 0,$$

$$\dot{P}_f\big|_{P_f=0} = 0,$$

$$\dot{P}_r\big|_{P_r=0} = \delta P_f \geq 0 \quad \text{for all } \delta \geq 0 \text{ and } P_f \geq 0.$$

This means that whenever one of the variables reaches zero, its time derivative is either strictly positive or zero, provided that $\lambda > 0$, $\delta \geq 0$, and $P_f \geq 0$. As a result, the variables cannot become negative, proving that the set $\mathbb{R}^3_+$ is positively invariant under the system dynamics.

Therefore, the model's solutions remain within the non-negative domain, which ensures that the system behaves consistently with physical reality. This positive invariance guarantees that the modeled dynamics respect natural constraints and allow for a meaningful interpretation in terms of pipe conditions and water flow in the network.

We now establish the boundedness of the system's solutions. To this end, let us define the total population of pipes as:

$$S(t) = P_b(t) + P_f(t) + P_r(t).$$

By summing the three differential equations of the model, we obtain:

$$\dot{S} = \lambda - (\gamma + \alpha)P_b - \theta P_f - \mu P_r.$$

Since $\gamma+\alpha, \theta, \mu$ are strictly positive, we can deduce:

$$\dot{S} \leq \lambda - \kappa S,$$

where $\kappa = \min\{\gamma+\alpha, \theta, \mu\}$. Solving this differential inequality gives:

$$\limsup_{t\to\infty} S(t) \leq \frac{\lambda}{\kappa},$$

which guarantees that $P_b(t)$, $P_f(t)$, and $P_r(t)$ are uniformly bounded for all $t > 0$.

3.2. Equilibrium Analysis. Understanding equilibrium states in water distribution systems provides critical insights into their long-term behavior. These stable configurations emerge when the system reaches a balance—where the number of pipes in good condition, those leaking, and those under repair remain constant over time. This balance isn't inherently good or bad; it simply reveals how the network behaves under current conditions. Some equilibria represent ideal scenarios with minimal water loss, while others expose vulnerabilities where leaks persist despite intervention efforts.

The real value of this analysis lies in its predictive power. By calculating these equilibrium points, we can anticipate whether existing maintenance strategies will gradually reduce leaks or allow them to accumulate. Certain thresholds become apparent—points beyond which leaks become inevitable without significant changes to repair rates, pipe quality, or detection methods. For instance, an equilibrium dominated by leaks signals that minor adjustments won't suffice; systemic changes are needed to shift the network toward a more sustainable state.

This isn't just abstract modeling. Equilibrium analysis lets us test real-world decisions before implementing them. What happens if we increase the repair budget by 15%? How much would upgrading leak sensors improve outcomes? The answers guide resource allocation, showing which interventions create meaningful change and which fall short. Sometimes, the results are sobering—revealing that certain equilibria (like chronic leakage) can't be eliminated without fundamental redesigns.

Beyond numbers, this approach reframes how we manage infrastructure. Instead of reacting to individual leaks, it highlights the bigger picture: how pipe aging, repair efficiency, and detection speed interact to shape the network's fate. Small tweaks in one area can tip the system from a leak-prone equilibrium to a stable, efficient one—or vice versa.

For utilities, this translates to smarter decisions. Knowing where tipping points lie helps prioritize investments before crises erupt. Recognizing that a modest boost in preventive maintenance could avert a downward spiral justifies proactive spending. Equilibrium analysis doesn't just diagnose problems; it illuminates pathways to resilience, turning reactive patchwork into strategic, long-term solutions.

An equilibrium point is defined as a situation where the system's rate of change becomes zero, indicating a stable state. These points are found by solving the following system of equations:

$$\lambda - (\gamma+\alpha)P_b - \beta P_b P_f = 0 \tag{4}$$

$$\beta P_b P_f - (\delta+\theta)P_f = 0 \tag{5}$$

$$\delta P_f - \mu P_r = 0 \tag{6}$$

We can identify two types of equilibrium: the leak-free equilibrium and the endemic equilibrium.

Equation (5) can be rewritten in factored form as:

$$[\beta P_b - (\delta+\theta)]P_f = 0,$$

which implies:

$$P_f = 0 \quad \text{or} \quad \beta P_b = \delta+\theta.$$

If $P_f = 0$, then $P_r = 0$ and $P_b = \frac{\lambda}{\gamma+\alpha}$. Thus, the equilibrium point

$$E_0\left(\frac{\lambda}{\gamma+\alpha},\, 0,\, 0\right)$$

represents a *leak-free state* in the network.

In the case where $P_f \neq 0$, we obtain:

$$P_b = \frac{\delta+\theta}{\beta}.$$

Solving equation (4) together with equation (5), we derive:

$$P_f = \frac{\lambda\beta - (\gamma+\alpha)(\delta+\theta)}{\beta(\delta+\theta)}.$$

By substituting this value into equation (6), we express P_r as:

$$P_r = \frac{\lambda\beta\delta - \delta(\gamma+\alpha)(\delta+\theta)}{\mu\beta(\delta+\theta)}.$$

We then define the *basic reproduction number* as:

$$R_0 = \frac{\lambda\beta}{(\gamma+\alpha)(\delta+\theta)}.$$

If $R_0 > 1$, the system admits a unique endemic equilibrium point E^*, given by:

$$E^*\left(\frac{\delta+\theta}{\beta}, \frac{\lambda\beta-(\gamma+\alpha)(\delta+\theta)}{\beta(\delta+\theta)}, \frac{\lambda\beta\delta-\delta(\gamma+\alpha)(\delta+\theta)}{\mu\beta(\delta+\theta)}\right).$$

This point corresponds to a *persistent leak state*, where the presence of leaks in the network remains stable over time.

Theorem 3.2.1.

(1) If $R_0 \leq 1$, the model admits a unique leak-free equilibrium:

$$E_0\left(\frac{\lambda}{\gamma+\alpha}, 0, 0\right),$$

which describes a scenario in which no persistent leaks are present in the network.

(2) If $R_0 > 1$, the model admits a unique endemic equilibrium:

$$E^*\left(\frac{\delta+\theta}{\beta}, \frac{\lambda\beta-(\gamma+\alpha)(\delta+\theta)}{\beta(\delta+\theta)}, \frac{\lambda\beta\delta-\delta(\gamma+\alpha)(\delta+\theta)}{\mu\beta(\delta+\theta)}\right).$$

representing a steady state in which leaks persist and continue to propagate.

4. Local Stability of Equilibrium Points

Understanding the behavior of water distribution networks near their equilibrium points is essential for effective and sustainable infrastructure management. Examining local stability allows us to assess how the system responds to small perturbations. Practically speaking, if the equilibrium is stable, the network is capable of recovering from minor disturbances, such as fluctuations in flow rates or temporary delays in repair activities, gradually returning to its steady operating state. Conversely, if the equilibrium is unstable, even minimal disruptions may amplify over time, leading to accelerated pipe deterioration and increasing water losses.

This stability analysis is not merely a theoretical exercise; it constitutes a valuable decision-making tool for infrastructure managers. By determining whether an equilibrium state can be

sustained autonomously or whether corrective interventions are necessary, we can prevent the system from drifting towards undesirable and costly conditions. The core of this analysis relies on the Jacobian matrix, which captures the local interactions between the system's components. The eigenvalues of this matrix are particularly insightful: when the real parts are negative, disturbances tend to decay, indicating a stable system; when positive, they signal an unstable system where disruptions are likely to escalate. These insights provide a scientific basis for designing monitoring strategies and optimizing maintenance schedules.

To evaluate the local stability of the equilibrium points E_0 and E^*, we construct the Jacobian matrix J of the system. This matrix is obtained by calculating the partial derivatives of the system's differential equations with respect to the variables P_b, P_f, and P_r. The structure of the Jacobian matrix encapsulates the dynamic interactions between these variables, offering a robust framework for analyzing the system's local dynamics near equilibrium.

We define the Jacobian matrix J as follows:

$$J = \begin{bmatrix} \frac{\partial f_1}{\partial P_b} & \frac{\partial f_1}{\partial P_f} & \frac{\partial f_1}{\partial P_r} \\ \frac{\partial f_2}{\partial P_b} & \frac{\partial f_2}{\partial P_f} & \frac{\partial f_2}{\partial P_r} \\ \frac{\partial f_3}{\partial P_b} & \frac{\partial f_3}{\partial P_f} & \frac{\partial f_3}{\partial P_r} \end{bmatrix}$$

where the functions governing the system dynamics are:

$$f_1(P_b, P_f, P_r) = \lambda - (\gamma + \alpha)P_b - \beta P_b P_f,$$

$$f_2(P_b, P_f, P_r) = \beta P_b P_f - (\delta + \theta)P_f,$$

$$f_3(P_b, P_f, P_r) = \delta P_f - \mu P_r.$$

By computing the partial derivatives, we obtain the explicit Jacobian matrix:

$$J = \begin{bmatrix} -(\gamma + \alpha) - \beta P_f & -\beta P_b & 0 \\ \beta P_f & \beta P_b - (\delta + \theta) & 0 \\ 0 & \delta & -\mu \end{bmatrix}$$

Theorem 4.1. *The leak-free equilibrium E_0 is locally asymptotically stable if $R_0 < 1$, and unstable if $R_0 > 1$.*

Proof. To assess the local stability of E_0, we examine the eigenvalues of the Jacobian matrix evaluated at the equilibrium point

$$E_0 = \left(\frac{\lambda}{(\gamma+\alpha)},\ 0,\ 0 \right).$$

We compute the Jacobian matrix at E_0, denoted $J(E_0)$, by substituting $P_b = \frac{\lambda}{(\gamma+\alpha)}$, $P_f = 0$, and $P_r = 0$ into the general Jacobian matrix:

$$J(E_0) = \begin{bmatrix} -(\gamma+\alpha) & -\beta\frac{\lambda}{(\gamma+\alpha)} & 0 \\ 0 & \beta\frac{\lambda}{(\gamma+\alpha)} - (\delta+\theta) & 0 \\ 0 & \delta & -\mu \end{bmatrix}.$$

To find the eigenvalues, we solve the characteristic equation:

$$\det(J(E_0) - \sigma I) = 0,$$

where σ denotes the eigenvalues and I is the identity matrix.

The characteristic polynomial yields the following eigenvalues:

$$\sigma_1 = -\mu, \quad \sigma_2 = -(\gamma+\alpha), \quad \sigma_3 = \beta\frac{\lambda}{\lambda+\alpha} - (\delta+\theta) = (\delta+\theta)(R_0 - 1),$$

where the basic reproduction number is defined as:

$$R_0 = \frac{\lambda\beta}{(\gamma+\alpha)(\delta+\theta)}.$$

We analyze the sign of the real parts of the eigenvalues:

- If $R_0 < 1$, then $\sigma_3 < 0$, and all eigenvalues have negative real parts. Hence, E_0 is locally asymptotically stable.
- If $R_0 > 1$, then $\sigma_3 > 0$, and at least one eigenvalue has a positive real part. Therefore, E_0 is unstable.

In conclusion, the local stability of the leak-free equilibrium E_0 directly depends on the reproduction number R_0, which governs the threshold between stability and instability in the leak dynamics.

Theorem 4.2. *The endemic equilibrium E^* is locally asymptotically stable if $R_0 > 1$, and unstable if $R_0 < 1$*

Proof. The characteristic polynomial of the Jacobian matrix evaluated at E^*, denoted J_{E^*}, is given by:

$$\det(J_{E^*} - \sigma I_3) = 0,$$

where I_3 is the 3×3 identity matrix, and σ denotes the eigenvalues.

Substituting the coordinates of the endemic equilibrium $E^* = (P_b^*, P_f^*, P_r^*)$ into the Jacobian matrix, we obtain:

$$\det \begin{bmatrix} -(\gamma+\alpha) - \beta P_f^* - \sigma & -\beta P_b^* & 0 \\ \beta P_f^* & \beta P_b^* - \delta - \theta - \sigma & \delta \\ 0 & 0 & -\mu - \sigma \end{bmatrix} = 0.$$

Expanding the determinant yields the characteristic equation:

$$(\mu + \sigma)\left(\sigma^2 + a_1\sigma + a_2\right) = 0 \tag{7}$$

with:

$$a_1 = \gamma + \alpha + \beta P_f^* + \delta + \theta - \beta P_b^* = (\gamma+\alpha)R_0,$$

$$a_2 = (\gamma+\alpha)(\delta+\theta)(R_0 - 1).$$

It is immediately clear that $\sigma = -\mu$ is a negative real root of equation (7). The remaining roots are determined by solving the quadratic:

$$\sigma^2 + a_1\sigma + a_2 = 0. \tag{8}$$

If $R_0 > 1$, then $a_1 > 0$ and $a_2 > 0$. According to the Routh–Hurwitz criterion [4], this implies that all roots of equation (8) have negative real parts. Therefore, the endemic equilibrium E^* is locally asymptotically stable.

On the other hand, if $R_0 < 1$, then $a_2 < 0$, meaning that equation (8) admits a positive real root. In this case, E^* is unstable. This result indicates that when $R_0 < 1$, perturbations near the endemic equilibrium E^* tend to grow, reflecting the disappearance of persistent leakage conditions in the network.

5. Global Stability of Equilibrium

This section focuses on the global stability analysis of two equilibrium points, E_0 and E^*. While local stability examines small perturbations near equilibria, global stability determines whether all system trajectories converge to an equilibrium, irrespective of initial conditions. A similar approach to study global stability using Lyapunov methods was proposed by Li, Su, and Wang [5] for stochastic coupled systems on networks. The Lyapunov method is a classical tool for proving global stability in fluid networks, as demonstrated by Ye and Chen [6] in their analysis of water distribution systems. Their approach, based on constructing an adapted Lyapunov function, provides sufficient conditions to guarantee trajectory convergence toward a stable equilibrium.

We consider the following system:

$$\begin{cases} \dot{P}_b(t) = \lambda - (\gamma+\alpha)P_b(t) - \beta P_b(t)P_f(t), \\ \dot{P}_f(t) = \beta P_b(t)P_f(t) - (\delta+\theta)P_f(t). \end{cases}$$

Theorem 5.1. *The leak-free equilibrium E_0 is globally asymptotically stable when $R_0 < 1$.*

Proof. We consider the following Lyapunov function:

$$V(P_b,P_f) = P_b - P_{b_0} - P_{b_0}\ln\left(\frac{P_b}{P_{b_0}}\right) + P_f,$$

where $P_{b_0} = \frac{\lambda}{\gamma+\alpha}$ is the steady-state value of P_b at the equilibrium point E_0.

Clearly, $V(E_0) = 0$, and $V(P_b,P_f) > 0$ for all $P_b \geq 0$, $P_f \geq 0$, with equality if and only if $P_b = P_{b_0}$ and $P_f = 0$; that is, only at the equilibrium E_0.

Differentiating V with respect to time along the trajectories of the system, we obtain:

$$\dot{V} = \frac{dV}{dt} = -\frac{(\gamma+\alpha)}{P_b}(P_b - P_{b_0})^2 + P_f(\delta+\theta)(R_0-1).$$

Therefore, if $R_0 < 1$, then $\dot{V} < 0$ for all $(P_b,P_f) \neq (P_{b_0},0)$. Thus, the Lyapunov function V decreases strictly along all trajectories except at the equilibrium point. Hence, the equilibrium E_0 is globally asymptotically stable.

Theorem 5.2. *Suppose that $R_0 > 1$. Then, the endemic equilibrium $E^* = (P_b^*, P_f^*)$ is globally asymptotically stable.*

Proof. We consider the auxiliary function:

$$\Psi(x) = x - 1 - \ln x$$

and define a Lyapunov function of the form:

$$V(P_b, P_f) = P_b^* \cdot \Psi\left(\frac{P_b}{P_b^*}\right) + P_f^* \cdot \Psi\left(\frac{P_f}{P_f^*}\right),$$

which can be written explicitly as:

$$V(P_b, P_f) = P_b^*\left(\frac{P_b}{P_b^*} - 1 - \ln\left(\frac{P_b}{P_b^*}\right)\right) + P_f^*\left(\frac{P_f}{P_f^*} - 1 - \ln\left(\frac{P_f}{P_f^*}\right)\right).$$

It is clear that $V(E^*) = 0$, and $V(P_b, P_f) > 0$ for all $P_b > 0$, $P_f > 0$, with equality only at $P_b = P_b^*$, $P_f = P_f^*$, confirming that V is a valid Lyapunov function.

By computing the time derivative of V along the trajectories of the system, we obtain:

$$\dot{V} = (\gamma + \alpha)(P_b - P_b^*)\left(1 - \frac{P_b^*}{P_b}\right) + (\delta + \theta)(P_f - P_f^*)\left(1 - \frac{P_f^*}{P_f}\right).$$

We have:

$$\frac{P_b}{P_b^*} + \frac{P_b^*}{P_b} \geq 2, \quad \frac{P_f}{P_f^*} + \frac{P_f^*}{P_f} \geq 2,$$

which implies:

$$\dot{V} \leq 0.$$

Define the invariant set:

$$\Gamma = \left\{(P_b, P_f) \mid \dot{V}(P_b, P_f) = 0\right\}.$$

On Γ, the equalities hold only if:

$$P_b = P_b^*, \quad P_f = P_f^*.$$

Substituting into the system shows that the only invariant set in Γ is:

$$\Gamma = \{E^*\}.$$

Therefore, by LaSalle's Invariance Principle [7], we conclude that the endemic equilibrium E^* is globally asymptotically stable.

6. The Optimal Control Problem

6.1. Presentation of Controls. To mitigate the severe economic and environmental consequences of water loss, water utilities traditionally resort to large-scale, disruptive interventions such as replacing entire sections of the network or shutting down supply for extended periods [8]. While effective in the long term, these strategies often lead to significant social inconvenience, operational costs, and service interruptions for residents.

In contrast, more efficient and targeted strategies are increasingly being adopted. Advanced technologies—such as acoustic leak detection enhanced by analytics [9] and satellite-based monitoring for pinpointing water loss [10]—enable early detection of vulnerabilities and support precise intervention on critical network segments only.

A notable example is the approach taken by the utility company LYDEC in Casablanca, Morocco, which implemented a large-scale project combining network modelling, permanent monitoring, and prioritized rehabilitation. This strategy focused on pre-emptively addressing pipes with the highest risk of failure, thereby preventing leaks before they occur and significantly reducing water loss without resorting to widespread network shutdowns [11].

Following this direction and seeking for cost-effective control strategies, we propose an optimal control framework based on two types of complementary interventions:

The first control u_1 represents preventive actions aimed at reducing the occurrence and propagation of new leaks. In water distribution systems, prevention is often achieved through pressure management and proactive maintenance. For example, utilities such as Thames Water and Sydney Water have implemented advanced pressure control strategies to reduce stress on pipes and delay the formation of leaks [12, 13]. This control also represents regular inspection programs and asset management practices that strengthen pipe resilience, as highlighted in international water loss management guidelines [3,14]. By incorporating preventive measures into the model, $u_1(t)$ reduces the effective leak transmission rate β, thereby protecting intact pipes (P_b) from being converted into leaking ones (P_f).

The second control u_2 represents the repair effort applied to leaking pipes. Unlike prevention, which aims to limit the occurrence of new leaks, this control acts in a reactive manner, once a leak has been detected. It reflects the intensity of active leakage management, a strategy

widely recognized as one of the most effective measures for reducing physical water losses [15, 16]. By increasing u_2, utilities can deploy additional teams, mobilize advanced leak detection technologies (such as acoustic sensors or satellite monitoring), and prioritize interventions in critical zones [17]. These actions shorten the lifetime of leaks, directly reducing non-revenue water volumes and restoring system efficiency more rapidly. Thus, u_2 formalizes the operational decision to accelerate repairs and improve the responsiveness of water utilities.

Based on these considerations, we introduce the two control variables u_1 and u_2, leading to the following controlled model:

$$\dot{P}_b = \lambda - (\gamma+\alpha)P_b - \beta(1-u_1)P_bP_f \tag{7}$$

$$\dot{P}_f = \beta(1-u_1)P_bP_f - \delta u_2 P_f - \theta P_f \tag{8}$$

$$\dot{P}_r = \delta u_2 P_f - \mu P_r \tag{9}$$

6.2. Objective Functional. The main objective of this optimal control strategy is to reduce the number of faulty pipes $P_f(t)$, to control the evolution of the repaired pipes $P_r(t)$, and to minimize the overall costs of applying controls. Then, the problem is to minimize the objective functional given by

$$J(u_1,u_2) = \int_0^T \left[AP_f(t) + BP_r(t) + \tfrac{C_1}{2}u_1^2(t) + \tfrac{C_2}{2}u_2^2(t)\right] dt \tag{10}$$

where T is the final time horizon of the control strategy, and $A > 0$, $B > 0$, $C_1 > 0$, and $C_2 > 0$ are weight constants associated with the system states and the control costs.

The aim is to determine the optimal controls $u_1^*(t)$ and $u_2^*(t)$ such that

$$J(u_1^*,u_2^*) = \min_{u_1\in U,\, u_2\in V} J(u_1,u_2). \tag{11}$$

where U and V are the control sets defined by

$$U = \{u_1(t)\,|\,u_{1,\min} \le u_1(t) \le u_{1,\max}, 0 \le t \le T\} \tag{12}$$

$$V = \{u_2(t)\,|\,u_{2,\min} \le u_2(t) \le u_{2,\max}, 0 \le t \le T\} \tag{13}$$

with bounds satisfying

$$0 < u_{1,\min} < u_{1,\max} < 1, \quad 0 < u_{2,\min} < u_{2,\max} < 1. \tag{14}$$

6.3. Sufficient Conditions.

Theorem 6.1. *There exists an optimal control pair $(u_1^*, u_2^*) \in U \times V$ such that:*

$$J(u_1^*, u_2^*) = \min_{u_1 \in U, u_2 \in V} J(u_1, u_2) \tag{15}$$

under the dynamic constraints of the control system defined previously and the associated initial conditions.

Proof: Given that the system parameters are bounded and the study period is defined over a finite time interval, the state variables $P_b(t), P_f(t)$, and $P_r(t)$ remain uniformly bounded for every admissible control pair $(u_1, u_2) \in U \times V$. This boundedness ensures that the objective function $J(u_1)$ remains bounded on the set $U \times V$, implying that the infimum of the functional is finite. Therefore, there exists a sequence of controls $(u_1^n, u_2^n) \in U \times V$ such that:

$$\lim_{n \to \infty} J(u_1^n, u_2^n) = \inf_{(u_1, u_2) \in U \times V} J(u_1, u_2). \tag{16}$$

This sequence represents a series of interventions that brings the objective function value as close as possible to its infimum. The corresponding state trajectories, denoted $P_b^n(t), P_f^n(t), P_r^n(t)$, are also bounded over a finite time interval. According to the Bolzano-Weierstrass theorem, a convergent subsequence can be extracted. Thus, there exist limits $u_1^*, u_2^* \in U \times V$ and limit states P_b^*, P_f^*, P_r^* such that along this subsequence:

$$u_1^n \to u_1^*, \quad u_2^n \to u_2^*, \quad P_b^n \to P_b^*, \quad P_f^n \to P_f^*, \quad P_r^n \to P_r^*. \tag{17}$$

The convergence of these sequences implies that the limit states satisfy the dynamic equations of the system under the limit controls u_1^* and u_2^*, confirming the feasibility of this solution. The compactness of the admissible control sets guarantees that any bounded sequence has an accumulation point, ensuring the existence of an optimal pair.

Finally, the continuity of the objective function with respect to the controls and state trajectories allows us to conclude that the limit value of the functional coincides with the objective function evaluated at (u_1^*, u_2^*), thus demonstrating that this pair is indeed an optimal solution to the posed problem.

This completes the proof of the existence of an optimal control that minimizes the objective function while satisfying the system dynamics and imposed constraints.

6.4. Necessary Conditions. A discrete version of Pontryagin's maximum principle [18] is applied to determine the conditions required for the optimal control strategy [19]. Accordingly, we define the Hamiltonian function as

$$\begin{aligned}\mathscr{H}(t) = {} & AP_f + BP_r + \frac{C_1}{2}u_1^2 + \frac{C_2}{2}u_2^2 \\ & + \lambda_b(t)\left[\lambda - (\gamma+\alpha)P_b - \beta(1-u_1)P_bP_f\right] \\ & + \lambda_f(t)\left[\beta(1-u_1)P_bP_f - \delta u_2 P_f - \theta P_f\right] \\ & + \lambda_r(t)\left[\delta u_2 P_f - \mu P_r\right].\end{aligned} \tag{18}$$

Here, $\lambda_b(t)$, $\lambda_f(t)$, and $\lambda_r(t)$ are the adjoint variables associated with the state variables $P_b(t)$, $P_f(t)$, and $P_r(t)$, respectively. These variables reflect how sensitive the objective function is to variations in each state over time. They are essential in establishing the backward system that, together with the state equations and control laws, characterizes the optimal solution.

This Hamiltonian formulation will serve as the basis for deriving the adjoint system and the conditions under which the controls $u_1(t)$ and $u_2(t)$ are optimal.

Theorem 6.2. *There exist adjoint variables $\lambda_b(t)$, $\lambda_f(t)$, and $\lambda_r(t)$ associated with the optimal state trajectories $P_b^*(t)$, $P_f^*(t)$, and $P_r^*(t)$, such that the following equations hold:*

$$\begin{aligned}\Delta\lambda_b(t) &= \lambda_b(\gamma+\alpha) + \lambda_b\beta(1-u_1)P_f - \lambda_f\beta(1-u_1)P_f, \\ \Delta\lambda_f(t) &= -A + \beta(1-u_1)P_b(\lambda_b-\lambda_f) + \lambda_f(\delta u_2+\theta) - \lambda_r\delta u_2, \\ \Delta\lambda_r(t) &= -B + \mu\lambda_r.\end{aligned} \tag{19}$$

with the transversality conditions:

$$\lambda_b(T) = 0, \quad \lambda_f(T) = 0, \quad \lambda_r(T) = 0,$$

and the optimal controls $u_1^*(t)$ and $u_2^*(t)$ are given by:

$$u_1^*(t) = \min\left\{u_{1,\max},\ \max\left\{u_{1,\min},\ \frac{\beta P_bP_f(\lambda_f-\lambda_b)}{C_1}\right\}\right\}, \tag{20}$$

$$u_2^*(t) = \min\left\{u_{2,\max},\ \max\left\{u_{2,\min},\ \frac{(\delta P_f(\lambda_f-\lambda_r)}{C_2}\right\}\right\}. \tag{21}$$

Proof: Using the discrete version of Pontryagin's maximum principle, we obtain the following adjoint equations:

$$\begin{aligned}
\Delta\lambda_b(t) &= -\frac{\partial \mathscr{H}}{\partial P_b} = \lambda_b(\gamma+\alpha) + \lambda_b\beta(1-u_1)P_f - \lambda_f\beta(1-u_1)P_f, \\
\Delta\lambda_f(t) &= -\frac{\partial \mathscr{H}}{\partial P_f} = -A + \beta(1-u_1)P_b(\lambda_b-\lambda_f) + \lambda_f(\delta u_2+\theta) - \lambda_r\delta u_2, \\
\Delta\lambda_r(t) &= -\frac{\partial \mathscr{H}}{\partial P_r} = -B + \mu\lambda_r.
\end{aligned} \tag{22}$$

with transversality conditions:

$$\lambda_b(T) = 0, \quad \lambda_f(T) = 0, \quad \lambda_r(T) = 0.$$

To derive the optimality conditions, we take the variation of the Hamiltonian with respect to the controls u_1 and u_2 and set the partial derivatives to zero:

$$\frac{\partial \mathscr{H}}{\partial u_1} = C_1u_1 + \beta P_bP_f(\lambda_b-\lambda_f) = 0 \quad \Rightarrow \quad u_1(t) = \frac{\beta P_bP_f(\lambda_f-\lambda_b)}{C_1} \tag{23}$$

$$\frac{\partial \mathscr{H}}{\partial u_2} = C_2u_2 + \delta P_f(\lambda_r-\lambda_f) = 0 \quad \Rightarrow \quad u_2(t) = \frac{(\delta P_f(\lambda_f-\lambda_r))}{C_2} \tag{24}$$

Finally, incorporating the control constraints, the optimal controls are expressed as:

$$u_1^*(t) = \min\left\{u_{1,\max},\ \max\left\{u_{1,\min},\ \frac{\beta P_bP_f(\lambda_f-\lambda_b)}{C_1}\right\}\right\}, \tag{25}$$

$$u_2^*(t) = \min\left\{u_{2,\max},\ \max\left\{u_{2,\min},\ \frac{(\delta P_f(\lambda_f-\lambda_r)}{C_2}\right\}\right\}. \tag{26}$$

7. Numerical Discretization and Simulation of the Model

We now present the numerical simulations for our optimal control problem concerning leak propagation in water networks. The model was implemented in MATLAB™, and the simulations were conducted using the parameter sets from Table 2 and Table 3, which together cover a range of typical and comparative scenarios for municipal pipe systems. The continuous-time system was first discretized using a forward Euler scheme, which allowed us to simulate the progression of pipe states—from good condition (P_b) to leaking (P_f) and then to repaired (P_r)—over discrete time intervals. An iterative optimization method was then used to solve the discretized system. In this process, the pipe state dynamics were computed forward in time,

while the repair strategies were updated to minimize the overall cost. The algorithm ran until successive solutions showed consistent results, indicating that a stable solution had been found.

This approach generated reliable temporal profiles for both pipe states and their corresponding maintenance schedules across different parameter sets. We analyze these results in the following sections.

Figure 1 illustrates two possible scenarios for the evolution of leaks in the network, depending on whether the basic reproduction number R_0 is below or above the critical threshold.

In subfigure (a), corresponding to a low leakage propagation regime ($R_0 = 0.22 < 1$), the system remains stable and manageable. The number of leaking pipes (P_f) initially experiences a slight increase but quickly peaks and then declines steadily. This indicates that the repair rate is sufficient to not only address new leaks but also to reduce the existing backlog. Consequently, the number of pipes in good condition (P_b) is largely preserved or even recovers over time. This represents a sustainable situation for a water utility, where the maintenance strategy is effectively containing the problem.

In stark contrast, subfigure (b) depicts a high propagation regime ($R_0 = 2.00 > 1$), where the network enters a state of escalating failure. Here, the number of leaking pipes (P_f) grows exponentially, quickly surpassing the number of intact pipes. This suggests that each existing leak is causing more than one new leak before it is repaired, leading to a cascade of failures. The stock of pipes in good condition (P_b) diminishes rapidly. This is a critical situation, demonstrating that the repair efforts are overwhelmed by the speed of deterioration. Without a significant intervention to either improve repair rates or reduce the leak propagation factor, the entire network risks a rapid descent towards widespread failure.

Figure 2 offers a different perspective on how the pipe network evolves over time, showing the relationship between intact pipes P_b and leaking pipes P_f regardless of the starting point. Each curve represents a possible trajectory for the network, depending on its initial state.

In subfigure (a), for $R_0 = 0.7$, we can see that all the paths, no matter where they begin, eventually converge to the leak-free equilibrium where $P_b^* = 5.0$ and $P_f^* = 0.0$. This visual

convergence of all trajectories provides clear numerical confirmation of Theorem 5.1, demonstrating the global asymptotic stability of the leak-free equilibrium E_0 when $R_0 < 1$. The system naturally returns to a leak-free state even after significant initial disturbances.

The situation changes completely in subfigure (b) $R_0 = 1.8$. Here, instead of converging to zero leaks, the trajectories are drawn toward the endemic equilibrium where $P_b^* = 2.78$ and $P_f^* = 0.44$. This pattern of all paths spiraling inward toward E^* numerically validates Theorem 5.2, confirming that the endemic equilibrium is globally asymptotically stable when $R_0 > 1$. The network inevitably reaches a state where leaks persist indefinitely, forming a stable, though undesirable, equilibrium.

Together, these phase portraits provide strong visual evidence for our analytical results. They show that R_0 acts as a precise threshold that determines the network's long-term fate, regardless of its initial condition. For utility managers, this means that calculating R_0 provides a definitive answer about whether their network can eventually become leak-free or is destined to maintain a persistent level of leakage.

Figure 3 provides a clear comparison between uncontrolled leak propagation and the effectiveness of our optimal control strategy. The side-by-side visualization helps understand exactly what we gain by implementing controlled maintenance.

In subfigure (a), where no control measures are applied, we see the natural progression of leaks in the network. The number of leaking pipes rises sharply, peaking at about 96 pipes around day 50. While some natural repair occurs over time, the process is slow, and a substantial number of leaks persist throughout the 200-day period. The intact pipes, shown in blue, decrease significantly as the leaks spread, and while the repaired pipes gradually increase, they never quite catch up with the ongoing leakage problem.

When we look at subfigure (b), where the control strategy is active, the difference is immediately apparent. The maximum number of leaking pipes reaches only 58, which represents a 40% reduction compared to the uncontrolled case. More importantly, the system's evolution over time shows that leaks are not only contained at a lower level but also decline much more rapidly after peaking. The intact pipes maintain higher numbers throughout the crisis, and the repaired pipes show a steadier, more consistent growth pattern.

What these results suggest is that the control strategy does not just reduce the total number of leaks—it changes the entire dynamics of the system. By strategically timing repairs and allocating resources where they are most effective, we are able to break the cycle of leak propagation more efficiently. The network recovers faster and maintains better overall health, even though it experiences the same initial challenge.

For water utility managers, this translates to concrete benefits: lower peak demand on repair crews, reduced water loss, and a quicker return to normal operations. The 40% reduction in maximum leaks is particularly important because it is during these peak periods that maintenance teams become overwhelmed and water losses become most severe.

Figure 4 examines how the leak propagation rate β influences the long-term behavior of our pipe network, comparing scenarios with and without control measures. These surface plots provide a comprehensive view of how different combinations of time and leak propagation rates affect the number of leaking pipes in the system.

In subfigure (b), where no controls are applied, we can see how sensitive the system becomes to changes in β. When β remains low, the number of leaking pipes stays manageable throughout the 200-day period. However, as β increases, the surface rises steeply, creating what looks like a growing ridge of leaks. This ridge not only reaches higher values but also persists longer over time, showing that networks with higher leak propagation rates struggle to recover naturally. The persistence of this ridge demonstrates how quickly a deteriorating network can move toward crisis when leak propagation goes unchecked.

Turning to subfigure (a), where our control strategy is active, the difference is quite noticeable. The surface remains much flatter across all values of β, and the persistent ridge seen in the uncontrolled case largely disappears. While higher β values still lead to more leaks—which is expected since the fundamental physics of leak propagation cannot be eliminated—the control strategy successfully contains the damage. Notably, the control not only reduces the peak number of leaks but also accelerates the recovery process, as evidenced by the quicker return to lower leak levels over time.

What these surfaces really show us is that our control strategy provides a form of ”resilience” against variations in leak propagation rates. Networks with aggressive leak propagation will

always be more challenging to manage, but the control approach provides a consistent level of protection regardless of how rapidly leaks spread. For water utilities dealing with different pipe materials or soil conditions that affect leak propagation, this suggests that the same control strategy could be effectively applied across various parts of their network.

Figure 5 explores how the repair rate δ influences the evolution of leaking pipes in our network, comparing the system's behavior with and without our control strategy. These surface plots help us understand how different repair capabilities affect the network's ability to handle leaks over time.

Looking first at subfigure (b), where no control measures are applied, we can see the natural limitation of repair efforts alone. When δ is very low, meaning repairs happen slowly, the number of leaking pipes grows substantially and remains high throughout the simulation. As δ increases, the surface gradually slopes downward, which is expected—faster repairs should lead to fewer leaks. However, even at relatively high repair rates, there is still a noticeable ridge of leaks that persists over time. This suggests that working faster alone has diminishing returns when the propagation of leaks through the network is not also addressed.

When we examine subfigure (a), where the control strategy is active, the relationship between repair rate and leak prevention becomes much more effective. The entire surface remains at lower levels across all repair rates, and the persistent ridge observed in the uncontrolled case largely disappears. Interestingly, the control strategy appears to make repair efforts more productive—each unit of repair capacity delivers better results in terms of leak reduction. The surface shows a smoother, more consistent decline in leaks as repair rates improve, without the diminishing returns seen in the uncontrolled scenario.

What these results suggest is that our control strategy does not replace repair efforts but rather complements them. By strategically deploying repairs where they can most effectively break the chain of leak propagation, we make the existing repair capacity work smarter. For water utilities facing budget constraints that limit how quickly they can repair leaks, this means that implementing an optimal control approach could help achieve better results with the same repair resources. The control strategy appears to provide the most value when repair capacity is limited, although it improves outcomes across the entire range of repair rates we tested.

Figure 6 provides perhaps the most important visual summary of our entire study—it shows exactly where the boundary lies between a manageable leak situation and one that could spiral out of control. The surface represents how the basic reproduction number R_0 changes as we vary both the leak transmission rate β and the repair rate δ.

What we are looking at is essentially a landscape of risk. The red region, where the surface rises above the critical plane, represents combinations of high leak propagation and slow repairs that lead to persistent leakage problems. In this zone, each leak creates more than one new leak before it is fixed, so the problem grows over time. The blue region below the plane shows the safer territory where leaks naturally die out because repairs outpace new leak formation.

The curved boundary between these two regions—that critical $R_0 = 1$ threshold—tells us something very useful about how these two factors interact. Notice how it is not a straight line. When repair rates are very low, it does not take much leak propagation to push the system into the danger zone. But as repair capabilities improve, the system can tolerate much higher leak propagation rates without tipping into the persistent leakage regime. This curved relationship means that improving repairs provides disproportionate benefits—each unit of improvement in repair rates allows the network to handle progressively more aggressive leak propagation.

For someone managing a real water network, this surface becomes a practical decision-making tool. If the typical leak propagation rate of the network is known—which might depend on pipe materials, soil conditions, and water pressure—you can see exactly how fast leaks need to be repaired to keep the system in the safe blue zone. Conversely, if budget constraints limit how quickly repairs can be performed, the graph shows the maximum leak propagation rate the network can tolerate before problems become self-sustaining.

This ultimately brings us back to why our control strategy matters. The goal of any intervention should be to move real-world systems from the red zone to the blue zone, either by reducing the effective leak propagation rate through better pipe maintenance or by making repairs more efficient through optimized scheduling. This surface illustrates all the possible ways to achieve that goal, providing water utilities with multiple pathways to maintain a sustainable network.

TABLE 2. Parameter values for the pipe failure model simulations

(A) Case 1: $R_0 < 1$

Parameter	Value
λ	0.2
γ	0.02
α	0.01
β	0.01
δ	0.1
θ	0.05
μ	0.03

(B) Case 2: $R_0 > 1$

Parameter	Value
λ	0.2
γ	0.02
α	0.01
β	0.03
δ	0.05
θ	0.05
μ	0.03

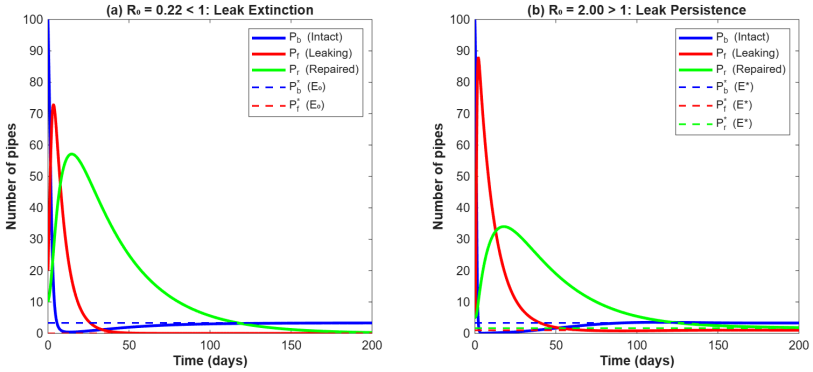

FIGURE 1. Comparing the dynamics of the model for two different values of R_0.

TABLE 3. Parameters and equilibrium values for the pipe failure model

(A) Case 1: $R_0 < 1$

Parameter	Value
λ	0.15
γ	0.02
α	0.01
β	0.021
δ	0.1
θ	0.05
$P_b(0)$	Varied
$P_f(0)$	Varied
R_0	0.7
P_b^*	5.0000
P_f^*	0.0000

(B) Case 2: $R_0 > 1$

Parameter	Value
λ	0.15
γ	0.02
α	0.01
β	0.054
δ	0.1
θ	0.05
$P_b(0)$	Varied
$P_f(0)$	Varied
R_0	1.8
P_b^*	2.77778
P_f^*	0.4444

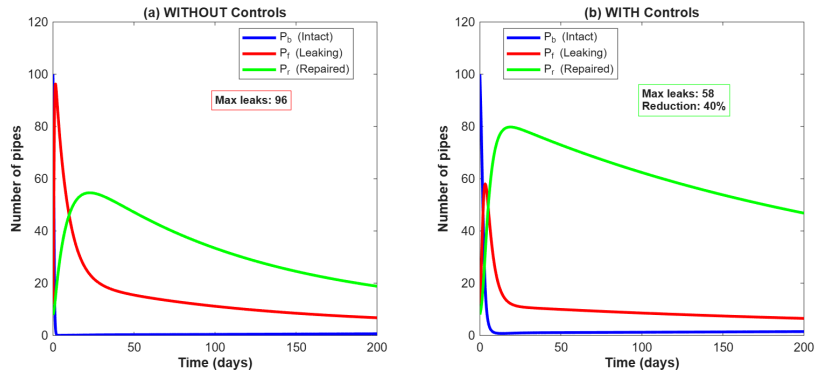

FIGURE 2. Dynamic of pipe systems with and without controls. (a) Behavior of intact (P_b), leaking (P_f), and repaired (P_r) pipes without controls. (b) Behavior with control strategies u_1 and u_2.

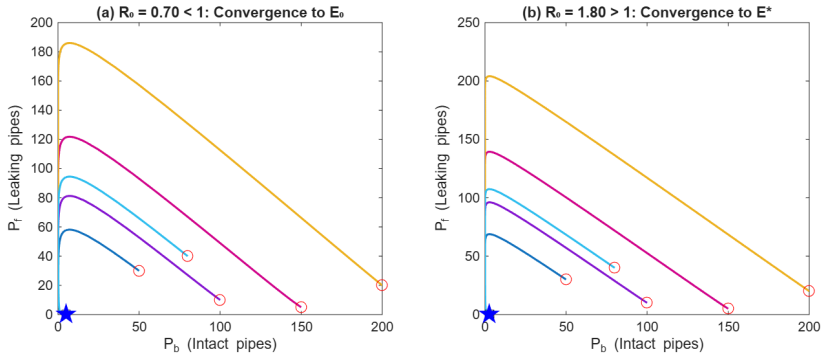

FIGURE 3. Phase portrait analysis demonstrating R_0-dependent stability in the pipe failure model.

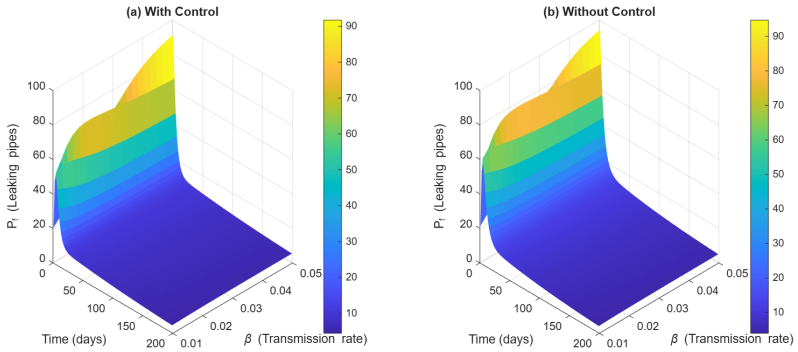

FIGURE 4. Amount of leaking pipes as function of time and β parameter. (a) Simulation with control u_1 and u_2. (b) Simulation without controls.

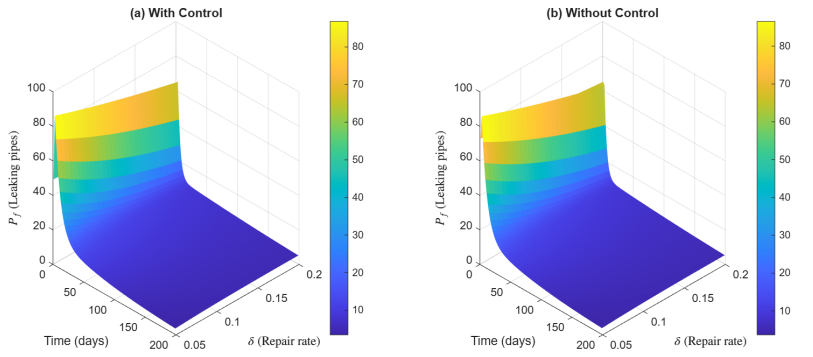

FIGURE 5. Amount of leaking pipes as function of time and δ parameter. (a) Simulation with control u_1 and u_2. (b) Simulation without controls.

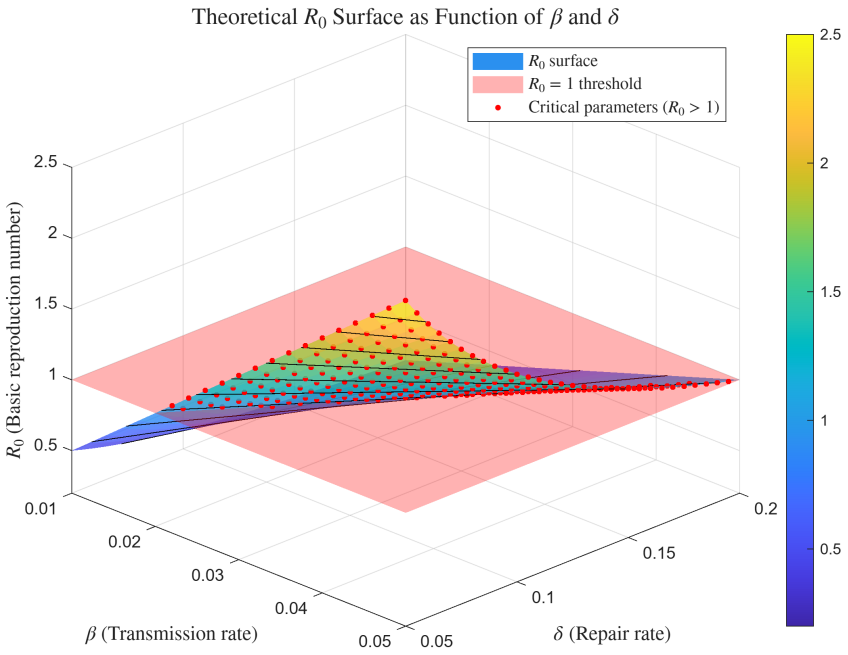

FIGURE 6. Theoretical analysis of basic reproduction number R_0 as function of transmission rate β and repair rate δ. The critical plane $R_0 = 1$ separates the domains of leak extinction ($R_0 < 1$) and leak persistence ($R_0 > 1$).

8. CONCLUSION

This study has addressed the critical problem of leak propagation in water distribution systems by proposing an innovative modeling approach inspired by compartmental models used

in epidemiology. By categorizing pipes into three distinct states—intact, leaking, and repaired—we have captured the fundamental dynamics of pipe deterioration and leak spread, offering a systemic perspective that goes beyond traditional detection methods.

The main contributions of this work are multiple. On the theoretical side, we established that the basic reproduction number R_0 acts as a critical threshold determining the long-term behavior of the network. Our stability analysis, both local and global, rigorously demonstrated that for $R_0 < 1$, the network inevitably converges to a leak-free state, whereas for $R_0 > 1$, it stabilizes in an endemic equilibrium where leaks persist. On the practical side, we designed and validated an optimal control strategy combining preventive and corrective actions, demonstrating its effectiveness in reducing the peak number of leaks by up to 40% and significantly accelerating network recovery.

The central message of this research is that leak management should be approached as controlling a complex dynamic system, rather than merely responding to isolated incidents. The parameter R_0 emerges as a powerful diagnostic indicator, allowing utility managers to quickly assess the vulnerability of their infrastructure. The risk landscapes we visualized, showing the $R_0 = 1$ threshold as a function of propagation and repair rates, provide an intuitive decision-making map to guide investments.

Concretely, a network manager can use our framework to assess whether their system is fundamentally manageable ($R_0 < 1$) or requires structural interventions ($R_0 > 1$). They can then simulate the impact of different strategies, for example, by comparing the effectiveness of investing in leak prevention (reducing β) versus strengthening repair capacities (increasing δ).

Although this model represents a significant step forward, it also opens several avenues for future research. A natural extension would be to incorporate pipe heterogeneity (materials, ages, diameters) and varying soil conditions. Enhancing the model with real-time pressure and flow data could also lead to even more effective adaptive control algorithms. Finally, a thorough economic study would help precisely quantify the return on investment of the proposed strategies.

In conclusion, this work demonstrates the value of interdisciplinary dialogue between epidemiology and infrastructure engineering. By translating a complex physical problem into a

proven mathematical framework, it provides utilities with both conceptual and practical tools to improve the resilience and sustainability of vital water networks.

CONFLICT OF INTERESTS

The authors declare that there is no conflict of interests.

REFERENCES

[1] Global Water Intelligence, Plugging the Leak: Innovative Solutions for Reducing Water Loss and Its Economic Impact, Industry Report, Global Water Intelligence, (2022).

[2] W.O. Kermack, A.G. McKendrick, A Contribution to the Mathematical Theory of Epidemics, Proc. R. Soc. Lond. Ser. A 115 (1927), 700–721. https://doi.org/10.1098/rspa.1927.0118.

[3] R. Puust, Z. Kapelan, D.A. Savic, T. Koppel, A Review of Methods for Leakage Management in Pipe Networks, Urban Water J. 7 (2010), 25–45. https://doi.org/10.1080/15730621003610878.

[4] I.S. Gradshteyn, I.M. Ryzhik, Routh-Hurwitz Theorem, Academic Press, (2000).

[5] W. Li, H. Su, K. Wang, Global Stability Analysis for Stochastic Coupled Systems on Networks, Automatica 47 (2011), 215–220. https://doi.org/10.1016/j.automatica.2010.10.041.

[6] H.Q. Ye, H. Chen, Lyapunov Method for the Stability of Fluid Networks, Oper. Res. Lett. 28 (2001), 125–136. https://doi.org/10.1016/s0167-6377(01)00060-8.

[7] J.P. LaSalle, The Stability of Dynamical Systems, SIAM, Philadelphia, (1976).

[8] H. Mala-Jetmarova, N. Sultanova, D. Savic, Lost in Optimisation of Water Distribution Systems? A Literature Review of System Design, Water 10 (2018), 307. https://doi.org/10.3390/w10030307.

[9] S. El-Zahab, E.M. Abdelkader, A. Fares, T. Zayed, Comparative Analysis of Machine Learning Techniques in Enhancing Acoustic Noise Loggers' Leak Detection, Water 17 (2025), 2427. https://doi.org/10.3390/w17162427.

[10] ASTERRA, The Hidden Cost of Water Loss: How Satellite-Based Leak Detection Saves Municipal Budgets Millions, (2025). https://asterra.io/resources/the-hidden-cost-of-water-loss-how-satellite-based-leak-detection-saves-municipal-budgets-millions.

[11] D. Loudyi, S. Azzaoui, F. Taghlabi, Improving Leakage Detection in Urban Water Distribution System: A Pilot Site for Smart Monitoring and Data Analysis in Casablanca City, Morocco, in: Proceedings of the 39th IAHR World Congress, Granada, 2022.

[12] M. Farley, S. Trow, Losses in Water Distribution Networks, IWA Publishing, (2003).

[13] J. Thornton, R. Sturm, G. Kunkel, Water Loss Control, McGraw-Hill, (2008).

[14] American Water Works Association, M36 Water Audits and Loss Control Programs, 3rd ed., American Water Works Association, (2009).

[15] M. Farley, G. Wyeth, Z. Ghazali, A. Istandar, S. Singh, The Manager's Non-Revenue Water Handbook: A Guide to Understanding Water Losses, United States Agency for International Development USAID, (2008).

[16] A. Lambert, W. Hirner, Losses from Water Supply Systems: Standard Terminology and Performance Measures, IWA Publishing, (2000).

[17] P. Fanner, J. Thornton, R. Sturm, J. Thornton, Leakage Management Technologies, IWA Publishing, (2007).

[18] L.S. Pontryagin, V.G. Boltyansky, R.V. Gamkrelidze, E.F. Mischenko, The Mathematical Theory of Optimal Processes, Interscience Publishers, New York, (1962).

[19] S.P. Sethi, What Is Optimal Control Theory? in: Optimal Control Theory, Springer Texts in Business and Economics, Springer, Cham, (2021). https://doi.org/10.1007/978-3-030-91745-6_1.

[20] E. Farah, I. Shahrour, Water Leak Detection: A Comprehensive Review of Methods, Challenges, and Future Directions, Water 16 (2024), 2975. https://doi.org/10.3390/w16202975.

[21] T. Gebhard, B.J. Sattler, J. Gunkel, M. Marquard, A. Tundis, Improving the Resilience of Socio-Technical Urban Critical Infrastructures with Digital Twins: Challenges, Concepts, and Modeling, Sustain. Anal. Model. 5 (2025), 100036. https://doi.org/10.1016/j.samod.2024.100036.

[22] H. Jiao, Z. Hu, Z. Yang, W. Zeng, F. Xu, et al., Hierarchical Structure-Based Model for Importance and Reliability Assessment of Water Distribution Networks, Reliab. Eng. Syst. Saf. 253 (2025), 110542. https://doi.org/10.1016/j.ress.2024.110542.

[23] A. Yazdani, P. Jeffrey, Water Distribution System Vulnerability Analysis Using Weighted and Directed Network Models, Water Resour. Res. 48 (2012), 2012WR011897. https://doi.org/10.1029/2012WR011897.